# Performance of a Broad-Band Acoustic Doppler Current Profiler

Blair H. Brumley, Ramon G. Cabrera, Kent L. Deines, and Eugene A. Terray

*Abstract*—**A new broad-band acoustic Doppler current profiler (ADCP) is described, with a useful range comparable to that of a commercially available narrow-band (incoherent) system of the same acoustic frequency, but having enhanced performance. The extra performance may be traded off among 1) reduced velocity variance, 2) reduced averaging time, and 3) finer depth resolution. This improvement permits the observation of phenomena with smaller time and space scales than is now possible with available ADCP's. An expression predicting rms velocity error in terms of system parameters and the measured acoustic data is given and is shown to be consistent with the independently measured velocity error among redundant beams. Two major sources of bias error in incoherent ADCP's are shown to be much reduced for the broad-band system. Field data demonstrating the improved performance over the existing incoherent ADCP is shown for cases of both strong and weak shear.**

*Keywords*—**Doppler, current profiler, current meter, sonar.**

## I. Introduction

RD Instruments (RDI) is currently developing a new generation of acoustic Doppler current profilers (ADCP's) that use broad-band signal processing techniques to improve the measurement performance beyond that of existing incoherent (narrow-band) ADCP's. The improvements may be translated into reduced velocity variance, shorter averaging times, and/or finer depth resolution. The development project began in 1985 through a small business innovative research (SBIR) program funded by the Office of Naval Research. Phase I of the project, proving the feasibility of the concept, was completed in 1986. Phase II, which involved the construction and testing of two prototypes, was completed in 1989. At the present, RDI is actively working on Phase III, the actual commercialization of the system. In the sections that follow we present a brief description of the broad-band technique and its relationship to similar technologies, followed by some of the test results.

## II. The Broad-Band Doppler Sonar

Ocean currents can be measured remotely using acoustic Doppler technique, a relatively new technology that has been used and proven in a variety of commercial, academic, and military applications. Commercially available ADCP's now exist that can measure currents over ranges up to several hundred meters with accuracies as good as or better than most of the traditional intrusive flowmeters. Existing ADCP's operate at a variety of frequencies, from tens of kilohertz to several megahertz. Low-frequency ADCP's are commonly used in open-ocean applications where long profiling range is required. High-frequency ADCP's, on the other hand, are used in shallow-water applications where depth resolution and resolving short spatial and temporal scales are important. In general, as the frequency of the ADCP increases, the current measurements are more precise (less short-term variability) or they can be obtained from smaller depth cells, at the expense of range reduction due primarily to increased sound absorption at higher frequencies. Several attempts have been made to overcome these limitations, that is, to develop a system that combines the long-range capability of low-frequency ADCP's with the resolution and precision of high-frequency systems. The broadband ADCP (BBADCP) is the first system to succeed in achieving such improved performance. The line of reasoning that we followed to arrive at this method is described below, starting with incoherent Doppler sonars, then the pulse-to-pulse coherent Doppler, and finally the broad-band Doppler sonar.

## III. Incoherent Doppler Sonar

Conventional incoherent (or narrow-band) ADCP's estimate the Doppler shift from the echoes of single-pulse pings. The somewhat misleading term "incoherent," short for "pulse-to-pulse incoherent," refers to the assumption that the echoes from separate pings are uncorrelated. The echoes are time gated to define range cells, each centered at slant range $(1/2)ct$, where $c$ is the speed of sound and $t$ is the time since the center of the transmit pulse. The width of the gate $T_a$ is usually matched to the pulse length $T_p$, giving a range resolution of $L = (1/2)cT$, where $T = T_a = T_p$. The Doppler shift is estimated by locating the spectral peak of thereturning signals from a given range cell. The estimation can be done either in the frequency domain by computing the spectrum of the signal and then picking the peak, or in the time domain using the covariance (or "pulse-pair") method to compute an estimate of the first moment of the power spectrum. The accuracy is limited in the first case by the spectral resolution and signal bandwidth, and (equivalently) in the second case by observation time and echo decorrelation, the latter primarily attributable to replacement of scatterers contributing to the echo as the pulse moves along the beam. All four of these limitations are determined by $T$ if $T_a = T_p$, with longer pulses giving more accuracy.

A lower bound on the single-ping standard deviation of the

Manuscript received June 6, 1991.

B. H. Brumley, R. G. Cabrera, and K. L. Deines are with RD Instruments, San Diego, CA 92131.

E. A. Terray is with the Department of Applied Ocean Physics and Engineering, Woods Hole, MA 02543.

IEEE Log Number 9102206.

0364-9059/91/1000-0402$01.00 

radial (beam-axis) velocity estimate using the incoherent Doppler technique is given by the Cramér–Rao bound, which for an unbiased estimator can be approximated by [1]

$$\sigma_{Ur} = \left[c\lambda/(8\pi L)\right]\sqrt{1 + 36/\mathrm{SNR} + 30/\mathrm{SNR}^2} \quad (1)$$

where SNR is the signal-to-noise ratio of the Doppler return. The noise bandwidth in the SNR of (1) is defined as the signal bandwidth $1/T$, rather than the actual noise bandwidth of the optimal filter.

In practice, the Cramér–Rao bound is not achieved. Often (1) is used with an empirical coefficient of about 1.4 to provide an rms error estimate for actual measurements. At large SNR, the product of range resolution and the empirically observed velocity error per ping is therefore typically

$$L\sigma_{Ur} = (1.4/8\pi)c\lambda. \quad (2)$$

This product is constant for fixed system frequency. The resolution–velocity error trade-off is the most serious limitation of incoherent Doppler systems, and is directly responsible for the long averaging times required to control the absolute velocity error. For example, a monostatic 300 kHz ADCP, profiling over 250 m in range cells of 2-m slant range, pinging twice a second, requires a 3.4-min average to reduce the Cramér–Rao bound on the standard error of the estimate of the velocity along the beam to 1 cm/s. With multiple beams at 30° to the vertical, the standard deviation of the measured horizontal velocity component increases by a factor of $1/(\sqrt{2}\sin 30°) \simeq 1.4$, doubling the required averaging time to achieve 1 cm/s rms error to nearly 7 min.

## IV. Pulse-to-Pulse Coherent Doppler Sonar

In pulse-to-pulse coherent systems, often called "coherent" or "pulse-coherent" for short, a series of short single-pulse pings is transmitted, and phase changes are observed from ping to ping at each range cell. The time $T_0$ between pings is adjusted to minimize interference from earlier pings, so the system effectively listens to the echo from only one pulse at a time. By sampling the echo from each pulse at fixed range so that the samples all correspond to the same set of scatterers, the pulse length $T_p$ no longer determines the spectral bandwidth, or equivalently, the decorrelation time scale, as it does in the raw received signal. The spectral bandwidth is greatly reduced, the factor being of the order of the Mach number, giving a remarkable decrease in velocity variance compared to incoherent systems.

Because pulse-to-pulse coherent systems are sampled, velocities are aliased about the Nyquist frequency of the sampling, which leads to the well-known "range–velocity" ambiguity:

$$U_{\max} R_{\max} \le \lambda c/8. \quad (3)$$

For example, for a 300-kHz system transmitting pulses separated by 10 m (two-way travel), the maximum range is somewhat less than 10 m and the unambiguous velocity interval is ±9 cm/s. Although this interval can be increased by using a nonperiodic pulse train, experience has shown that a factor of order 5 is a practical limit [2]. As a consequence, conventional pulse coherent systems have been limited to relatively short ranges, of order tens of meters.

The Doppler frequency of the sampled signal can be estimated by spectral analysis, or the covariance ("pulse-pair") method. The velocity error was analyzed by Miller and Rochwarger [3] for independent sample pairs. For this case, they showed that the covariance estimator is also maximum likelihood, and in the limit of large SNR found the Doppler velocity error per pair to be independent of ping spacing:

$$\sigma_{Ur} = (1/2)\lambda\sigma_f = 2^{-3/2}\lambda B \quad (4)$$

where $B$ is the Doppler bandwidth in Hertz. The decorrelation time is $(2\pi B)^{-1}$, assuming a Gaussian-shaped autocorrelation function $e^{-(2\pi B\tau)^2/2}$ where $\tau$ is time lag. Equation (4) is similar to (2) for incoherent sonars, where $B = 1/T = (1/2)c/L$.

The independent-pair assumption of Miller and Rochwarger [3] is rarely valid in practical applications, however. In the more general case where successive pairs are correlated, which was analyzed by Zrnic [4], the velocity variance tends to be inversely proportional to the observation time-bandwidth product rather than the number of independent sample pairs. In the case of large SNR, large decorrelation time $1/2\pi B \gg T_0$, and even larger observation time $MT_0$, the error in the average radial velocity from $M$ pings is:

$$\sigma_{Ur} = (1/2)\lambda\sigma_f = \left(\pi^{-1/4}/4\right)\lambda B/\sqrt{MT_0 B}\,. \quad (5)$$

Since the pulse length $T_p$ does not affect the error at high SNR's, a transmit pulse need contain only a few cycles of the carrier, and range resolutions of order 10 cm are easily attainable. For example, $L$ = 10 cm at 300 kHz corresponds to a 40-cycle pulse.

The product $\lambda B$ tends to be nearly independent of system frequency, typical values ranging from 0.3 to 10 cm/s. In contrast to incoherent sonars, the spectral bandwidth $B$ and decorrelation time $(2\pi B)^{-1}$ are not determined by the pulse length $T_p$, but rather the remaining sources of phase noise. The most important of these are: turbulence within the sample volume, beam divergence, finite scatterer residence time, and acceleration during the averaging period [5]. Roughly speaking, $\lambda B$ is usually proportional to the larger of the rms turbulent velocity fluctuation within the range cell or the cross-beam velocity component multiplied by the beam width (in radians).

These decorrelation effects set an upper limit on the time between pings ((5) no longer holds for large $T_0$). For example, a decorrelation time of 20 ms typical of a 300-kHz system corresponds to a range of only 15 m. RDI's initial efforts towards developing high-resolution pulse-coherent Doppler current profilers consisted of a 1200-kHz monostatic unit intended for profiling over a 10-m range; but it became obvious that echo decorrelation made it impossible to obtain data for a pulse separation as large as 20 m (twice the maximum range). Reducing the frequency to 300 kHz increased the echo decorrelation time by a factor of four, making measurements possible. The constraints on maximum

ping separation imposed by velocity ambiguity and decorrelation time may result in additional decorrelation due to echo interference (also called "self-noise" or "range ambiguity"). If backscatter strength is not uniform, echoes from beyond the profiling range can be of sufficient strength to overpower echoes from within the profiling range [6], [7].

## V. Broad-band Doppler Sonar

The problems of the pulse-to-pulse coherent sonar with range-velocity ambiguity, echo decorrelation, and vulnerability to backscatter strength variability could be greatly reduced if the system were freed from the constraint that the time between pulses be greater than the propagation time to the maximum range. This is accomplished in the broad-band Doppler sonar by simultaneously receiving echoes from two or more pulses. By shortening the interval between pulses relative to that typical of a pulse-to-pulse coherent system, the maximum unambiguous velocity can be increased. However, the spacing between pings (sets of pulses) can now be as large as necessary to cover the desired range. Range is only limited by the SNR, rather than by the Nyquist sampling constraint (3).

The broad-band Doppler sonar can be thought of as a compromise combining the best features of the incoherent and the pulse-to-pulse coherent sonars: the robustness and large range of the former and the improved spatial resolution and low variance of the latter. The practical spatial resolution and velocity variance that can be achieved is generally intermediate between the two methods.

No attempt is made to actually separate the simultaneously received echoes from the pulses. The covariance method [4] is simply used to correlate echoes from different pulses scattering from the same range cell. The phase of the autocorrelation function of the complex demodulated signal at a lag corresponding to the pulse spacing is proportional to the velocity. Echoes from different parts of the water column are uncorrelated, so they do not cause bias. However, self-noise from the uncorrelated echo in each member of the sample pair *does* reduce the correlation coefficient significantly. When two pulses are used, samples of the received signal contain returns from two distinct range cells, and samples separated by the pulse spacing only have one range cell in common. Self-noise due to the echoes from range cells one pulse-spacing to each side of the common range cell cuts the correlation coefficient approximately in half, compared to a pulse-to-pulse coherent system.

If two pure-tone pulses are used at a spacing $T_0$ matching the pulse length so there is no gap between them, the system is equivalent to a single incoherent pulse whose length is twice the pulse spacing. Now suppose we shorten the pulses by a large factor while maintaining the same pulse spacing and averaging interval (range cell size) as before. The effect of shortening the pulses is to shorten the correlation time of the echo, or equivalently, to broaden its bandwidth. We still have to accept a signal-to-self-noise ratio of 1 (a correlation coefficient of 1/2), but variance per ping is reduced in proportion to the averaging time-bandwidth product, which is equal to the ratio $T_a / T_p$ of the range cell length to the pulse length. In contrast, both the incoherent and coherent systems as commonly implemented use $T_a = T_p$, so the time-signal bandwidth product is only 1. (This is not to be confused with $MT_0B$ in (5).)

Unfortunately, cavitation and shock cause Doppler sonars to be peak power limited. Reducing the pulse length at constant peak power causes a drastic reduction in transmitted energy, echo SNR, and hence profiling range. Phase coding solves this problem by allowing the same transmitted energy as an uncoded pulse while giving echoes with a bandwidth nearly as wide as that of echoes from short pulses only one code element in length. It is not necessary to decode (or pulse compress) the received signal, so long as the same code is used for each pulse. The biphase codes now used are chosen by brute-force computer search to have low autocorrelation sidelobes (except at lag $T_0$). If the pulse length is chosen equal to the range cell size, the time-bandwidth product is approximately equal to the length of the code $M_a$. The reduced variance of the broad-band system compared to the incoherent system is attributable to both the increased time-bandwidth product and to the larger time lag $T_0$ over which phase changes can be observed.

The manner in which the covariance method extracts velocity information from the received echoes can be understood in either the frequency domain or the time domain. In the frequency domain, the power spectrum of the received echo from a pair of pulses with spacing $T_0$ is a fine comb (raised cosine) modulating a broad spectral envelope, the frequency spacing of the teeth being $1/T_0$ and the total number of teeth corresponding roughly to the pulse spacing-bandwidth product. The Doppler effect causes a stretching of this spectrum, the fractional displacement being approximately twice the Mach number. We do not measure the Doppler shift in the centroid of the spectrum as in an incoherent system, but rather the shift in the position of the teeth of the comb.

The broad-band system is perhaps more easily understood from the point of view of the time domain. Doppler time distortion can be thought of as causing a shift in the delay between echoes of successive pulses from the same scatterers, regardless of the frequency content of the pulses. The autocorrelation magnitude function of a pair of broad-band pulses is a three-peaked structure, the center of the side-peak occurring at a lag corresponding to the echo delay. The fractional Doppler shift in the position of the side peak from $T_0$ is approximately twice the Mach number. Measuring the side peak position from the autocorrelation magnitude alone is unambiguous but noisy. The phase at the center of the side-peak (referred to the demodulation local oscillator frequency) gives a more precise measure of its shift, subject to ambiguity at intervals of $2\pi$.

Fig. 1 compares the minimum estimation variance (Cramér–Rao lower bound) attainable for a given SNR for both conventional incoherent Doppler (1) and two-pulse broad-band systems using several time-bandwidth products (code lengths) $M_a$ [5]. The on-center pulse separation of the broad-band system has been set equal to the range cell size $L$. In this plot, the SNR is the SNR that would be measured

by the respective instruments, each with its own bandwidth. Hence the horizontal axis, $SNR \times M_a$, is directly related to range. $M_a$ is 1 for the incoherent system.

The important feature to notice in Fig. 1 is that although the performance of the broad-band systems degrades very rapidly at low SNR, it is always superior to the incoherent system over the latter's useful range (roughly $SNR \times M_a >$ 15 dB). The broad-band system shows more range-dependence in its performance over this range, however. At high SNR, gains of roughly 10 to 100 in the velocity variance are theoretically possible.

The expression given by Zrnic (equation (B7) of [4]) for the variance of velocity estimates using the covariance method can be generalized without modification to the case where the sample pair spacing is many sample periods, rather than just one. For the broad-band method, $T_0$ is set equal to the pulse spacing. A simplified form of Zrnic's equation for the one-beam variance per ping of the radial velocity $U_r$ derived from the radial Doppler frequency $\omega_r$ for a two-pulse transmission is:

$$\begin{aligned}\operatorname{var}(\pi U_r/U_a) &= \operatorname{var}(\omega_r T_0) \\ &= (C^2(2M_a))\left[\rho^{-2} - 1 \right. \\ &\quad \left. + 2\max(0, 1 - T_0/T_a)\right] \qquad (6)\end{aligned}$$

where

$$U_a = (1/4)\lambda/T_0 \qquad (7)$$

is the radial half-lane ambiguity velocity corresponding to a phase of $\pi$, $T_a$ is the averaging interval (usually $T_a \leq T_0$ and the final term vanishes), and $M_a = T_a/T_e$ is the number of code elements per averaging interval. $C$ is a coefficient incorporating nonideal aspects of the code and signal processing as well as correlation between sequential samples ($C \simeq$ 1.4 and 2.0 for the first and second prototypes, respectively, and 1.5 for recent models). The factor $M_a/C^2$ can be considered the effective time-bandwidth product, indicating the amount of averaging that goes into the one-ping velocity estimate for each range cell.

The autocorrelation coefficient magnitude $\rho$ at lag $T_0$ can be estimated from the data. It can also be estimated theoretically from:

$$\rho = \rho_{\text{ideal}}\beta/(1 + 1/\text{SNR}) \qquad (8)$$

where $\rho_{\text{ideal}} = (1 - 1/N_p)$, or 1/2 for $N_p = 2$ pulses, is the ideal autocorrelation coefficient for a particular transmitted code, and SNR is the signal-to-noise ratio as ordinarily defined (total echo power:noise power). The coefficient $\beta$ represents the net effect of various factors that cause decorrelation, including the four discussed above for pulse-to-pulse coherent sonars (see [5] for formulas), and also nonuniform echo strength. Nonuniform echo strength is important at short range and near sharp changes in scattering strength. Beam divergence and residence-time effects (the former generally dominating) are proportional to the cross-beam velocity, and so are important in shipboard applications.

Equation (6) allows us to analyze possible performance trade-offs among velocity variance, averaging time, and depth

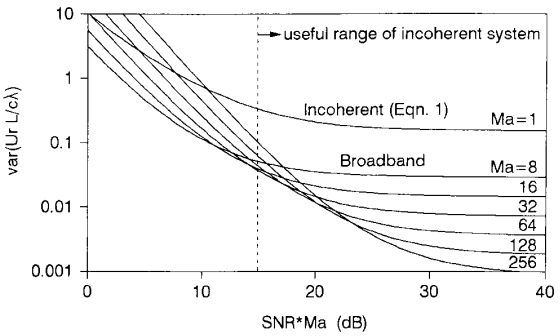


Fig. 1. Cramér-Rao lower bound on velocity variance, comparing two-pulse broad-band systems of various code lengths with an incoherent system of the same range cell size and pulse length (half the total transmission length).

resolution. Suppose that the ambiguity velocity $U_a$ is constrained to $\pm 40$ cm/s. This limits the on-center pulse separation $1/2cT_0$ to 470 wavelengths (1 m vertical at 600 kHz). Except in unusual circumstances, the errors in consecutive pings are uncorrelated, so the velocity variance is inversely related to the number of pings averaged. Equation (6) shows that it is also inversely related to $M_a$, the number of code elements per range cell. At 600 kHz with 8 cycles per code element, there will be 118 code elements per vertical meter. Equation (6) with $M_a = 118$, $\rho = 1/2$, and $C = 1.5$ predicts a single-ping standard deviation of 2 cm/s in the radial velocity, or 3 cm/s in the horizontal (with multiple 30° beams). This could be cut by roughly a factor of 2 by averaging over four pings, by averaging one ping over 4 m, or by averaging two pings over 2 m (neglecting the last term in Equation 6). Alternatively, the bandwidth could be increased by a factor of 4 (perhaps with a higher transmit frequency) so that there would be four times as many code elements per meter, but this parameter is generally fixed for a particular instrument.

Two of the most important sources of bias in the incoherent ADCP are virtually eliminated in the broad-band system. Because the bandwidth of the incoherent ADCP is small compared with typical Doppler shifts, a tracker is usually used to keep the echo signal spectrum centered in the filter passband. Bias can occur when strong velocity shear causes the tracker to lag and the signal spectrum to shift toward one side of the passband, which is not perfectly flat. The broad-band ADCP requires no tracker because the bandwidth is large compared to typical Doppler shifts. It is not subject to the same type of bias due to uneven spectral weighting because it does not measure the first moment of the spectrum. A second source of bias is noise, which is colored by the receiver filters. In both instruments, the noise bandwidth is not much greater than the signal bandwidth. However, the broadband ADCP measures the phase of the autocorrelation function at a lag much farther from the central noise peak than the incoherent ADCP does, making it immune to that particular type of bias.

Since we demonstrated the broad-band method with our first prototype, Robert Pinkel and his colleagues [8] have independently developed a "hybrid coded mode" using mul-

tiple pulses for their Doppler sonars that is essentially identical in principle to the broad-band system described above, although it differs slightly in the details of its implementation.

## VI. Preliminary Test Results

Initial tests verified the improved variance performance when the bandwidth is increased. An example of the results of such a test using the first prototype, a 300-kHz broad-band system in Lake Miramar, is Fig. 2, showing the standard deviation of the radial velocity as a function of bandwidth. The standard deviation was estimated from the variance of vertical differences between range bins (apparent shear) over 64 consecutive pings. The range cell size, pulse length, and pulse separation were all kept constant at 1.9 slant m, while each pulse was divided into more and more code elements. The bandwidth shown is the number of code elements transmitted per second during the transmit pulse. This test verified that the variance is indeed proportional to the reciprocal bandwidth, as predicted by (6).

Measurements from the deeper part of Massachusetts Bay taken during the Stellwagen Bank experiment with the second 300-kHz prototype provide a further test of (6). Fig. 3 shows a profile of the standard deviation of the error velocity (the difference between redundant vertical velocity estimates in orthogonal planes, in units equivalent to the one-beam radial velocity rms error) for a record of 512 consecutive pings. The heavy line represents the measured rms error, while the light solid line represents the predicted error using (6) with the value of the correlation coefficient magnitude $\rho$ given by the average of the measured values in the four beams. The dashed line is also a theoretical prediction, but with the theoretical value of $\rho$ from (8), with the SNR predicted by the sonar equation, and theoretical estimates of the various decorrelation effects used to estimate $\beta$. The transmitted signal was two back-to-back 1-m pulses of 120 code elements each. An incoherent system with the same 1-m range cells at the same frequency would have a minimum rms error velocity of about 35 cm/s. Fig. 3 shows that theoretical methods do a reasonable job of predicting error and range performance, despite a certain amount of unavoidable uncertainty in the scattering strength profile. Furthermore, it shows that by using the measured correlation magnitudes, the instrument can predict its own performance very accurately.

A direct comparison of a velocity time series from a 600-kHz broad-band ADCP with a 1200-kHz incoherent ADCP mounted side-by-side and pinging alternately is shown in Fig. 4. The curves shown represent the average velocity in a 1-m depth cell at at range of 5 m in Lake Miramar. Each sample point represents the average from 4 pings over 2 s. The standard deviation of the incoherent system is about six times that of the broad-band system, in spite of its higher frequency (and hence shorter range). No obvious difference in bias between the two systems is apparent in this figure. The distance traveled found by integrating each of the time series differs by less than 1 in 237 m, or 0.3%, not a statistically significant difference for this short record.

The Stellwagen Bank experiment afforded an opportunity to use the 300-kHz second prototype to gather data of scientific interest. The BBADCP was mounted on the side of the 14-m *R / V Asterias* along with a standard RDI 1200-kHz ADCP. The ADCP's were used in conjunction with an S4 electromagnetic current meter, 200-kHz echosounder, and CTD's. Stellwagen Bank is a sill where strong tidal forcing and seasonal stratification cause interesting internal hydraulic phenomena, including strong shears, shear-induced mixing, undular internal hydraulic jumps (lee waves), and the periodic launching of free internal wave trains [9]. Fig. 5 shows a stack plot of typical velocity profiles from that experiment, taken at slack tide at the change from flood to ebb (leftward to rightward flow). The horizontal axis is a dual axis, repre-

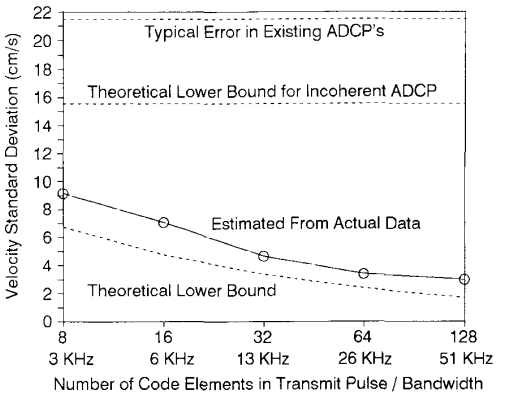


Fig. 2. Radial velocity error as a function of system bandwidth.

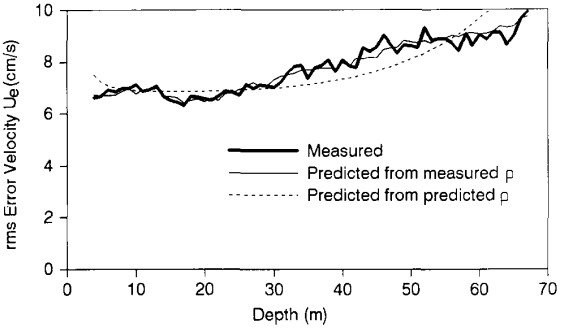


Fig. 3. Measured versus predicted error velocity. Average is over 512 pings.

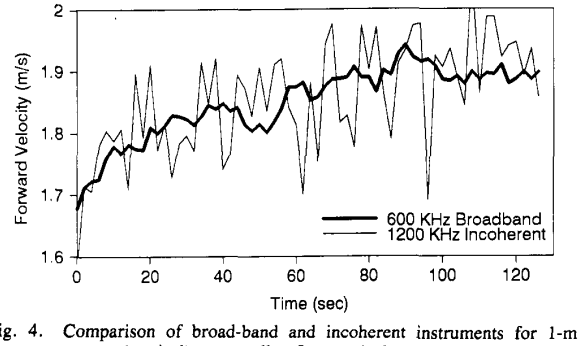


Fig. 4. Comparison of broad-band and incoherent instruments for 1-m (vertical) range cell at 5-m vertical range.

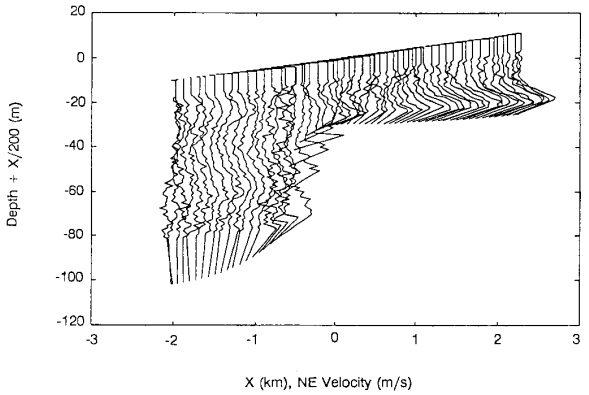


Fig. 5. Stack plot (waterfall plot) of the cross-sill velocity component at slack tide. Profile top and bottom ends have been extrapolated (see text).

senting both the position (in kilometers) of each profile from the crest of the sill along the northeastward-oriented transect across the sill, and also the velocity scale (in meters per second) for each profile of the cross-sill velocity component. Each profile ends at 0 m/s, both at top and bottom. Missing portions of each profile have been extrapolated, assuming uniform flow at the top where there was little stratification and a linear profile at the bottom, where the stratification was quite strong. (The bottom portion of each profile cannot be used since it is contaminated by the vertical bottom echo.)

The hydraulic jump, which had been several hundred meters to the left of the sill during flood tide, has dissipated and traveled to the right, so it is near the crest of the sill at the time of this transect. To the left of the sill in the deep water of Massachusetts Bay ($-1.5$ km), a complicated three-layer structure to the flow can be seen. Some of this flow seems to be unsteady. More striking is the strong near-bottom flow on the gently sloping right side of the sill, resulting in strong measured shear at about 2/3 of the depth and implying strong unmeasured shear in the bottom boundary layer. Gradient Richardson numbers measured in this region a few minutes before, using velocity profiles similar to Fig. 5 and density profiles from CTD measurements, were close to the value of 1/4 expected for an actively mixing stratified flow, suggesting that the remarkably strong shear measured by the broad-band ADCP was in fact physically reasonable.

## VII. Conclusions

The broad-band acoustic Doppler technique developed by RDI has been successfully proven through the construction and evaluation of several prototype instruments. Test results confirm that the technique indeed provides a reduction in the variance of the Doppler velocity estimates that is inversely proportional to the signal bandwidth, while maintaining the long-range profiling capability of incoherent ADCP's. A number of issues affecting the performance of the BBADCP, such as bias errors and velocity ambiguities, has been investigated and found to be manageable.

## References

[1] K. B. Theriault, "Incoherent multibeam Doppler current profiler performance: 1—Estimate variance," *IEEE J. Oceanic Eng.*, vol. OE-11, pp. 7-15, Jan. 1986.

[2] R. Lhermitte and R. Serafin, "Pulse-to-pulse coherent Doppler signal processing techniques," *J. Atmos. Oceanic Tech.*, vol. 1, pp. 293-308, 1984.

[3] K. S. Miller and M. M. Rochwarger, "A covariance approach to spectral moment estimation," *IEEE Trans. Inform. Theory*, vol. IT-18, pp. 588-596, 1972.

[4] D. S. Zrnic, "Spectral moment estimates from correlated pulse-pairs," *IEEE Trans. Aerosp. and Electron. Systm.*, vol AES-13, pp. 344-354, July 1977.

[5] R. Cabrera, K. Deines, B. Brumley, and E. Terray, "Development of a practical coherent acoustic Doppler current profiler," in *Proc. Oceans '87*, pp. 93-97, 1987.

[6] F. D. Rowe, K. L. Deines, and R. L. Gordon, "High resolution current profiler," in *Proc. IEEE Third Working Conf. Current Measurements*, G. F. Appell and W. E. Woodward, Eds. New York: IEEE Press, 1986, pp. 184-189.

[7] A. Lohrmann, B. Hackett, and L. P. Roed, "High resolution measurements of turbulence, velocity and stress using a pulse-to-pulse coherent sonar," *J. Atmos. Oceanic Tech.*, vol. 7, pp. 19-37, 1990.

[8] R. Pinkel and J. T. Sherman, "Acoustic Doppler measurement of internal waves: New techniques and observations," *J. Acoustical Society of America*, Supplement 1, vol. 87, 1990.

[9] T. K. Chereskin, "Generation of internal waves in Massachusetts Bay," *J. Geophys. Res.—Oceans*, vol. 88, pp. 2649-2661, 1983.

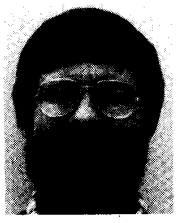

**Blair H. Brumley** received the Sc.B. degree from Brown University, Providence, RI in 1975, and the M.S. and Ph.D. degrees from Cornell University, Ithaca, NY in 1979 and 1984, respectively; all three degrees were in environmental engineering.

Since 1989 he has been a Research Scientist at RD Instruments, San Diego, CA. He spent the previous five years with the Applied Ocean Physics and Engineering Department (formerly known as the Ocean Engineering Dept.) at the Woods Hole Oceanographic Institution as a Postdoctoral Investigator, Postdoctoral Scholar, and Assistant Scientist. His research interests include turbulence, sediment transport, gas transfer, bubbles, high-frequency acoustics, and signal processing.

**Kent L. Deines** received the B.S. degree in 1967 and the M.S.E.E. in 1971 from San Diego State University.

He has been chief engineer of RD Instruments, a sonar development and manufacturing company in San Diego, since he and Fran Rowe started the company in 1982.

**Ramon G. Cabrera** received the B.S. in physics in 1979 from Univisidad Central de Venezuela, and two M.S. degrees, in ocean engineering in 1984 and computer science in 1985, from the University of Hawaii.

He was a research associate at the Joint Institute for Marine and Atmospheric Research (JIMAR) at the University of Hawaii from 1983 until 1987. Since then he has been Vice President of Engineering at RD Instruments, where he has worked on various advanced product development projects, including long-range coherent, high-resolution coherent, and broad-band Doppler and acoustic scintillation systems.

**Eugene A. Terray** for a photograph and biography, please see page 337 of this issue.